CHEMISTRY
A EUROPEAN JOURNAL

DOI: 10.1002/chem.200900799

Chiral Salan Aluminium Ethyl Complexes and Their Application in Lactide Polymerization

Hongzhi Du,[a, b, c] Aldrik H. Velders,[d] Pieter J. Dijkstra,[b, e] Jingru Sun,[a] Zhiyuan Zhong,[e] Xuesi Chen,*[a] and Jan Feijen*[b]

Abstract: Synthetic routes to aluminium ethyl complexes supported by chiral tetradentate phenoxyamine (salan-type) ligands [Al(OC_6H_2(R-6-R-4)CH_2)$_2${$CH_3N(C_6H_{10})NCH_3$}-C_2H_5] (**4**, **7**: R = H; **5**, **8**: R = Cl; **6**, **9**: R = CH_3) are reported. Enantiomerically pure salan ligands **1–3** with (*R*,*R*) configurations at their cyclohexane rings afforded the complexes **4**, **5**, and **6** as mixtures of two diastereoisomers (**a** and **b**). Each diastereoisomer **a** was, as determined by X-ray analysis, monomeric with a five-coordinated aluminium central core in the solid state, adopting a *cis*-(O,O) and *cis*-(Me,Me) ligand geometry. From the results of variable-temperature (VT) ^{1}H NMR in the temperature range of 220–335 K, ^{1}H–^{1}H NOESY at 220 K, and diffusion-ordered spectroscopy (DOSY), it is concluded that each diastereoisomer **b** is also monomeric with a five-coordinated aluminium central core. The geometry is intermediate between square pyramidal with a *cis*-(O,O), *trans*-(Me,Me) ligand disposition and trigonal bipyramidal with a *trans*-(O,O) and *trans*-(Me,Me) disposition. A slow exchange between these two geometries at 220 K was indicated by ^{1}H–^{1}H NOESY NMR. In the presence of propan-2-ol as an initiator, enantiomerically pure (*R*,*R*) complexes **4–6** and their racemic mixtures **7–9** were efficient catalysts in the ring-opening polymerization of lactide (LA). Polylactide materials ranging from isotactically biased (P_m up to 0.66) to medium heterotactic (P_r up to 0.73) were obtained from *rac*-lactide, and syndiotactically biased polylactide (P_r up to 0.70) from *meso*-lactide. Kinetic studies revealed that the polymerization of (*S*,*S*)-LA in the presence of **4**/propan-2-ol had a much higher polymerization rate than (*R*,*R*)-LA polymerization (k_{SS}/k_{RR} = 10.1).

Keywords: aluminum · chirality · lactide · polymerization · salan

Introduction

Poly(lactic acid)s (PLAs) prepared from renewable resources are important biodegradable materials for biomedical, pharmaceutical, and agricultural applications.[1] Although different methods for the synthesis of PLAs have been exploited, the most convenient is the ring-opening polymerization (ROP) of lactide (LA), the cyclic dimer of lactic acid. Current research in this area is particularly focused on the design and synthesis of single-site catalyst/initiators of gener-

[a] Dr. H. Du, Dr. J. Sun, Prof. Dr. X. Chen
Changchun Institute of Applied Chemistry
Chinese Academy of Sciences, Changchun 130022 (China)
Fax: (+86)431-85262112
E-mail: xschen@ciac.jl.cn

[b] Dr. H. Du, Dr. P. J. Dijkstra, Prof. Dr. J. Feijen
Department of Polymer Chemistry and BioMaterials
Faculty of Science and Technology
Institute for Biomedical Technology, University of Twente
7500 AE, Enschede (The Netherlands)
Fax: (+31)53-4892155
E-mail: J.Feijen@tnw.utwente.nl

[c] Dr. H. Du
Graduate School of Chinese Academy of Sciences
Beijing 100039 (China)

[d] Dr. A. H. Velders
Laboratory of Supermolecular Chemistry and Technology
University of Twente, 7500 AE, Enschede (The Netherlands)

[e] Dr. P. J. Dijkstra, Prof. Dr. Z. Zhong
Biomedical Polymers Laboratory and
Jiangsu Key Laboratory of Organic Chemistry
College of Chemistry, Chemical Engineering and Materials Science
Soochow University, Suzhou 215123 (China)

Supporting information for this article is available on the WWW under http://dx.doi.org/10.1002/chem.200900799.

al formula L_nMR,[2] in which M is a central metal atom, ligated with L_n, which represents an ancillary ligand. R is the initiating group covalently linked through a remaining vacant orbital. The steric and electronic properties of the ligand affect the activity and the stereoselectivity of the catalyst. Appropriate combinations of L_n with M and R have generated numerous catalyst/initiators containing Ca,[3] Al,[4] Zn or Mg,[5] Ti,[6] or Fe,[7] as well as the rare earth elements[8] as central metal atoms. Most of these catalysts are highly efficient and lactide polymerization proceeds in a well-controlled manner. Moreover, in certain cases stereoregular PLAs have been obtained from *rac*-LA [an equimolar mixture of (*S*,*S*)-LA and (*R*,*R*)-LA)] or *meso*-LA by use of these metal complexes.[9–11] Some recent breakthroughs in the stereoselective polymerization of lactide in the presence of rare earth metals complexed by achiral phenoxyamine ligands have been achieved by the groups of Carpentier[12] and Cui,[13] who have prepared highly heterotactic PLAs from *rac*-LA.

Tetradentate phenoxyamine ligands are usually referred to as salan-type ligands, which can be considered fully reduced Schiff base (salen) ligands (Scheme 1).[14] The salan-

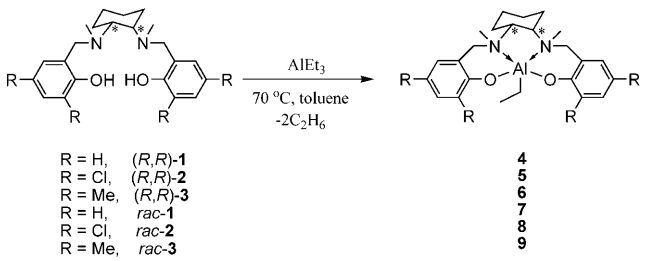

Scheme 1. Structures of salan ligands and their aluminium ethyl complexes. The configurations at the cyclohexane rings are either (*R*,*R*) or racemic mixtures of (*R*,*R*) and (*S*,*S*).

type ligands have more flexible structures than salen ligands, due to the sp^3 hybridization of their amine nitrogen atoms. A salan ligand containing a *trans*-1,2-diaminocyclohexane bridge may lead to various kinds of interesting chiral metal complexes. Recently, chiral Fe(salan),[15,16] Ti(salan),[17] and V(salan)[18] complexes have been studied and applied in the asymmetric oxidation of sulfides. Chiral Ti(salan)[19–21] complexes have been exploited in the asymmetric addition of metal alkyls to aldehydes, whereas Mo(salan)[22] complexes have been used in the enantioselective pinacol coupling of aryl aldehydes. Moreover, Kol and co-workers have demonstrated that chiral Zr(salan) complexes have the ability to initiate isospecific polymerization of hex-1-ene, 4-methylpent-1-ene,[23] or vinylcyclohexane,[24] as well as the cyclopolymerization of hexa-1,5-diene.[23]

The structures and catalytic applications of chiral Al(salan) complexes, however, have never been reported.[25] Previously, we described a chiral Jacobsen salen aluminium isopropoxide, which exerts significant stereocontrol in *rac*-LA polymerization, affording highly isotactic PLAs with P_i values of up to 0.93.[9c,d] In this paper we describe the synthesis and structures of chiral salan aluminium ethyl complexes with regard to their ligand wrapping modes, as well as to their catalytic behavior in lactide polymerization in the presence of propan-2-ol as an initiator.

Results and Discussion

Synthesis of chiral salan aluminium ethyl complexes: Enantiomeric (*R,R*)-1,2-diaminocyclohexane was obtained from *trans*-1,2-diaminocyclohexane by a procedure described by Larrow et al.[26] The synthesis of the ligand precursors (*R*,*R*)-**1** and *rac*-**1** (Scheme 1) was accomplished by a three-step procedure. Firstly, a condensation between racemic or (*R,R*)-1,2-diaminocyclohexane and salicylaldehyde (2 equiv) yielded the salen intermediate. Subsequent reduction of the imine bonds in the presence of an excess of $NaBH_4$ afforded the salan intermediate. The ligand precursors were obtained by condensation of the secondary amine groups with an excess of formaldehyde and reduction with an excess of $NaBH_4$ (Scheme S1 in the Supporting Information). The syntheses of the ligand precursors *rac*-**2**, (*R*,*R*)-**2**, *rac*-**3**, and (*R*,*R*)-**3** (Scheme 1) were carried out similarly, except that the salan intermediates were synthesized through Mannich condensations of 2,4-substituted phenols, formaldehyde, and racemic or (*R,R*)-1,2-diaminocyclohexane (Scheme S2 in the Supporting Information). All ligands were isolated as white crystalline solids in high yields after recrystallization from acetone.

Treatment of the enantiomeric pure salan ligand precursors (*R*,*R*)-**1**, (*R*,*R*)-**2**, or (*R*,*R*)-**3** with equimolar amounts of $AlEt_3$ in toluene at 70 °C resulted in the formation of salan aluminium ethyl complexes **4**, **5**, and **6**, respectively (Scheme 1). Interestingly, the ^{1}H NMR spectroscopic data for **4**, **5**, and **6** in [D_8]toluene at 295 K clearly revealed the presence of two species in each case. One species (**a**) gives a dissymmetric resonance pattern, whereas the other (**b**) gives a symmetric resonance pattern. The molar ratios of **a**/**b** in **4**, **5**, and **6** were 10:4, 10:2.5, and 10:3, respectively. As an example, in the ^{1}H NMR spectrum of **4** (Figure 1), the appearance of four doublets for the benzylic $ArCH_2$–NCH_3 protons at 3.70, 3.60, 3.19, and 2.71 ppm with a ^2J(H,H) coupling constant of 13.0 Hz, together with the two singlets at 1.84 and 1.72 ppm for the N–CH_3 protons (Figure 1, top), both indicated dissymmetric surroundings of these groups in the salan complex, which was denoted **4a**. On the other hand, the symmetric resonance pattern includes two doublets for the benzylic $ArCH_2$–NCH_3 protons appearing at 3.44 and 3.28 ppm with the same ^2J(H,H) value of 13.0 Hz and a singlet at 1.80 ppm for the N–CH_3 protons (Figure 1, top), and this complex was denoted **4b**. Moreover, the methylene protons in the aluminium ethyl groups in **4a** or **4b** displayed a significant difference in chemical shift (Figure 1, bottom), showing that these protons in **4a** or **4b** are all diastereotopic. Because of the *gem*-hydrogen effect, each quar-

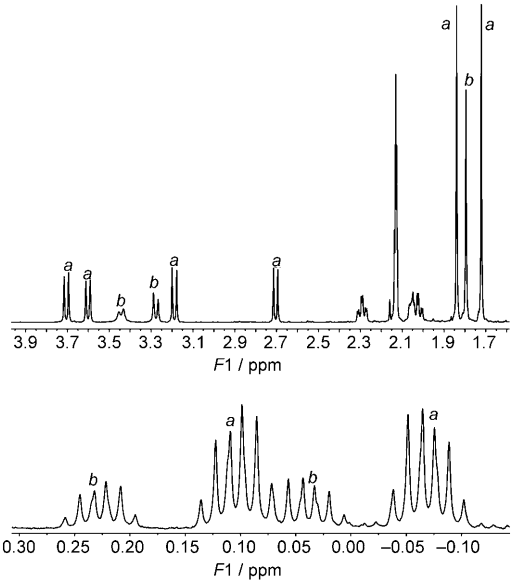

Figure 1. Expanded region of the ^{1}H NMR spectrum of **4**, indicating the presence of two diastereoisomers **a** and **b**. Top) 600 MHz, [D_8]toluene, 295 K, ArCH_2–NCH_3. Bottom) Al$CH_2$$CH_3$.

tet is spilt into an unresolved double quartet. The ^{1}H–^{1}H NOESY spectrum of **4** in [D_8]toluene at 295 K revealed no slow exchange between the species **4a** and **4b** on the NMR timescale (Figure S1 in the Supporting Information). Single crystals of **4a** were isolated from a saturated toluene solution at room temperature and characterized by X-ray analysis (Figure 2; for crystallographic data see Table 1). Despite several attempts, only single crystals of species **4a** were obtained.

Table 1. Crystallographic data for **4a** and **9a**.

	4a	**9a**
formula	$C_{24}H_{33}AlN_2O_2$	$C_{28}H_{41}AlN_2O_2$
crystal size [mm]	0.20×0.19×0.09	0.27×0.13×0.08
formula weight	408.50	464.61
cryst. syst.	monoclinic	monoclinic
space group	$P2_1$	$P2_1/c$
a [Å]	7.7422(10)	14.5190(12)
b [Å]	17.058(2)	14.5891(11)
c [Å]	8.7022(10)	12.3277(10)
α [°]	90	90
β [°]	100.678(2)	100.100(2)
γ [°]	90	90
V [Å^3]	1129.4(2)	2570.8(4)
Z	2	4
ρ_{calcd} [g cm^{-3}]	1.201	1.200
radiation (λ), [Å]	$Mo_{K\alpha}$ (0.71073)	$Mo_{K\alpha}$ (0.71073)
$2\theta_{max}$ [°]	26.05	26.08
μ [mm^{-1}]	0.112	0.106
F(000)	440	1008
no. of obsd reflns	6374	14235
no. of params refnd	265	305
GOF	1.050	1.017
R_1	0.0625	0.0583
wR_2	0.0731	0.1269

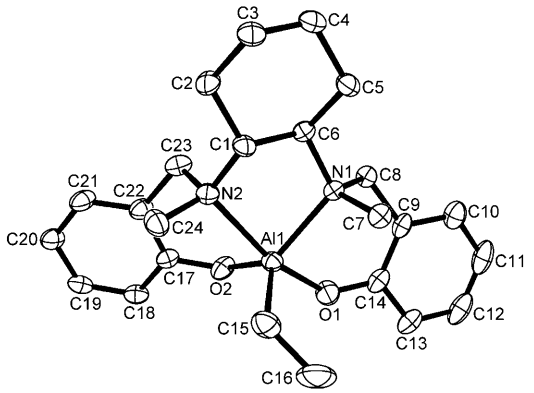

Figure 2. Molecular structure of **4a**; all hydrogen atoms are omitted for clarity.

The complex **4a** was monomeric with a five-coordinated central aluminium atom (Figure 2). The geometry around such a five-coordinated aluminium atom would ideally be square pyramidal or trigonal bipyramidal and can be expressed by a τ value, which is 0 in the case of an ideal square pyramidal (sqp) and 1 in that of an ideal trigonal bipyramidal (tbp) geometry.[27] The τ value of **4a** is 0.53, revealing a geometry intermediate between **A**, an ideal sqp, and **B**, an ideal tbp in this complex (Scheme 2, below). The τ value of **4a** is higher than that of the corresponding chiral salen aluminium methyl complex (τ = 0.35),[28] indicating a more flexible ligand geometry, as a result of the sp^3 hybridization of the tertiary amine nitrogen atoms in the salan complex. The two phenolic oxygen atoms exist in a *cis* arrangement relative to the central aluminium. The Al1–N1 [2.115(3) Å] and Al1–N2 [2.222(4) Å] bond lengths (Table S1 in the Supporting Information) are both in the 2.01–2.26 Å range, values generally observed for Al–N bond lengths in tetradentate salen aluminium ethyl complexes.[29] The two methyl groups on the nitrogen atoms are in a *cis* configuration relative to the five-membered ring formed by Al1, N1, N2, C1, and C6. The nitrogen atoms have become chiral, due to the coordination with Al. The configurations of the two nitrogen atoms are *R* for N2 and *S* for N1.

To clarify the structure of **4b** further, additional NMR characterization was performed. In ^{27}Al NMR, four-coordinated aluminium complexes give resonance signals at ~70 ppm, whereas five- or six-coordinated aluminium complexes give resonance signals at ~40 and ~0 ppm, respectively.[30] The ^{27}Al NMR spectrum of **4** did not exhibit any peaks in the −70 to 280 ppm range, perhaps due to the asymmetric coordination of the salan ligand around the aluminium center.[31] However, DOSY NMR measurements revealed that **4a** and **4b** have comparable diffusion coefficients, indicating similar effective molecular radii, and further demonstrating that **4b** is also monomeric. This also indicates that **4b** may be a diastereoisomer of **4a**. The VT ^{1}H NMR spectra of **4** ([D_8]toluene) in the 295–335 K temperature range did not reveal any tendency for the resonances of the benzylic ArCH_2–NCH_3 protons of **4b** to coalesce (Figure S2 in

the Supporting Information). This indicates that the two Al–N bonds in **4b** are stable at room temperature or even higher temperatures. The symmetric resonance pattern for the four benzylic ArCH_2–NCH_3 protons of **4b** at 295 K indicates that these protons are symmetrically arranged in the complex. From this information, either the highly symmetric sqp geometry **C** or the tbp geometry **D**, or even a geometric intermediate between **C** and **D**, was considered the most probable for **4b** (Scheme 2, below). Because of the presence of only one singlet for the *N*-methyl groups of **4b** at 295 K, it is assumed that the two *N*-methyl groups exist in a *trans* arrangement. To reveal the structure of **4b** fully, 1D and 2D NMR experiments were carried out.

Firstly, VT ^{1}H NMR analysis of **4** in [D_8]toluene was performed. With decreasing temperature the two doublets for the four benzylic ArCH_2–NCH_3 protons of **4b** seen at 295 K split into two doublets (partly overlapping) and a broad peak at 220 K (Figure 3). It is speculated that with a further decrease in the temperature this broad peak should also split into two doublets. Moreover, the singlet representing the N–CH_3 protons at 295 K split into two broad peaks at 220 K (Figure S3 in the Supporting Information).

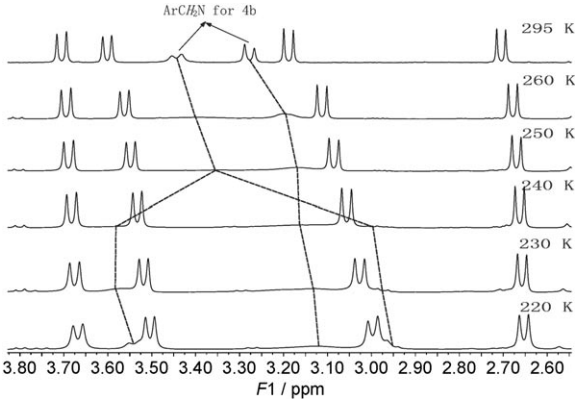

Figure 3. VT ^{1}H NMR spectra of **4** in [D_8]toluene between 220–295 K (ArCH_2–NCH_3 region).

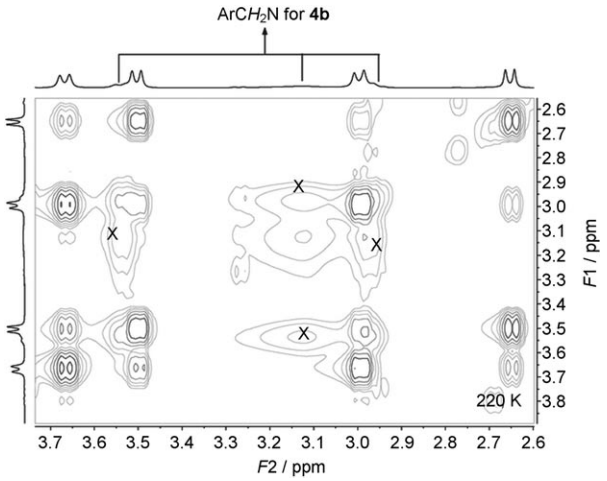

Figure 4. ^{1}H–^{1}H NOESY NMR spectrum of **4** at in [D_8]toluene 220 K (ArCH_2–NCH_3 region). Evidence for the exchange between the two geometries of **4b** is provided by the presence of additional exchange-NOE cross-peaks labeled X.

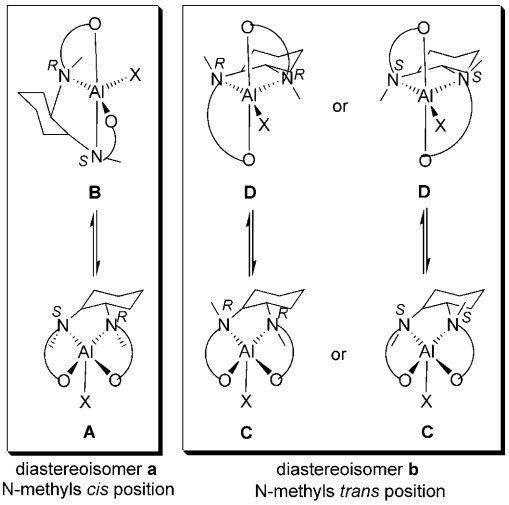

Scheme 2. Schematic representation of the geometries adopted by diastereoisomers **a** and **b**.

The ^{1}H–^{1}H NOESY NMR spectrum of **4** at 220 K displayed positive off-diagonal cross-peaks (with the diagonal cross-peaks phased in positive sign, and the NOE cross-peaks observed at opposite sign) between the ArCH_2–NCH_3 protons (Figure 4) as well as the N–CH_3 protons of **4b** (Figure S4 in the Supporting Information). All of these observations indicate that at 220 K a slow exchange takes place between two geometries of **4b**. From these data, it is assumed that diastereoisomer **4b** adopts a geometry intermediate between **C** and **D** with the *N*-methyl groups existing in a *trans* orientation (Scheme 2). At 295 K, diastereoisomer **4b** shows a fast exchange between the sqp geometry **C** and the tbp geometry **D** on the NMR timescale. At low temperatures, the exchange between these two geometries was slow enough to be observable by NMR. So far, however, we have not been able to conclude whether either the (*R*,*R*) or (*S*,*S*) configurations (with respect to the nitrogen centers) or even mixtures of the two are present in **4b** (Scheme 2).

On the basis of the NMR and X-ray analysis, it is reasonable to assume two different pathways by which these chiral salan aluminium ethyls were formed. Because the conformation of the cyclohexane ring is fixed upon formation of the five-coordinated aluminium complex, the positions of the methyl groups on the nitrogen atoms will also be fixed. Once the free ligand in the solution coordinates the aluminium atom with the *N*-methyl groups in a *cis* position, a wrapping mode with a *cis*-(O,O) geometry in-between **A** (sqp) and **B** (tbp) should be favored. The chiral salan ligand generates diastereoisomer **4a** with (*R*,*S*) chiral nitrogen centers. On the other hand, if the free ligand in the solution adopts a conformation with the *N*-methyl groups in a *trans* position, a geometry intermediate between **C** (sqp) and **D** (tbp) as in

diastereoisomer **4b** should be favored, with either (*R*,*R*) or (*S*,*S*)—or even both—configurations for the chiral nitrogen centers.

The salan aluminium complexes **7–9** were obtained from racemic mixtures of the ligands **1–3** (Scheme 1). Only single crystals of **9a** could be isolated from a saturated toluene solution at room temperature. X-ray analysis of **9a** (Figure 5; for crystallographic data see Table 1) revealed that the complex was also dissymmetric with a five-coordinated central aluminium atom as in **4a**. The packing modes in the unit cell of **9a** show that a racemate crystallization had occurred. A τ value of 0.90 is calculated, indicating a trigonal bipyramidal geometry with N1 and O2 occupying the axial positions, and N2, C17, and O1 located in the equatorial plane. The central aluminium atom deviates from the equatorial plane by ca. 0.201 Å in the direction of O2. The axial bond length for Al1–O2 [1.7931(18) Å] is slightly longer than that for its equatorial counterpart Al1–O1 [1.7631(17) Å]. Moreover, in relation to N2, placed in the equatorial plane with a bond length of 2.039(2) Å from Al1, the N1 atom located at the axial site is weakly coordinated to Al1 with a longer Al1–N1 distance [2.448(2) Å]. Similar weak interactions were also observed in an aluminium complex ligated by an achiral salan ligand reported by Gibson and co-workers[25] and in an aluminium complex stabilized by a 1,ω-dithiaalkanediyl-bridged bis(phenolate) ligand reported by Okuda et al.[4c] As in **4a**, the methyl groups on the nitrogen atoms exist in a *cis* arrangement relative to the five-membered ring formed by C6, C1, N2, N1, and Al1. The configurations of the two nitrogen atoms are *R* for N2 and *S* for N1.

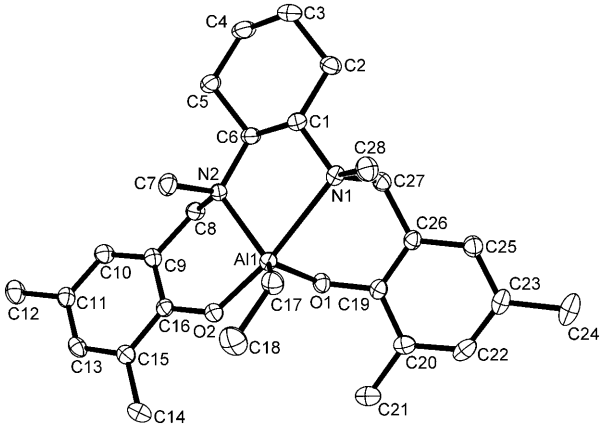

Figure 5. Molecular structure of **9a**; all hydrogen atoms are omitted for clarity.

Ring-opening polymerization of *rac*- and *meso*-LA in solution: Because it had so far not been possible to separate diastereoisomers **a** and **b**, complexes **4–6** and **7–9** were each treated with propan-2-ol (1 equiv) to generate the active isopropoxide initiators for the ROP of *rac*- or *meso*-LA in situ. All polymerizations were carried out in toluene at 70 °C, and the levels of conversion were monitored by ^{1}H NMR determination of samples withdrawn from the reaction mixtures. In the presence of propan-2-ol as an initiator, **4–6** and **7–9** furnished PLAs with similar number average molecular weights as calculated, as well as narrow molecular weight distributions, indicating well-controlled polymerization. Representative polymerization results are summarized in Table 2.

The tacticities of the resulting polymers were determined by inspection of the methine region in their homonuclear decoupled ^{1}H NMR spectra. Compound **4**/propan-2-ol and compound **7**/propan-2-ol polymerized *rac*-LA to form isotactically biased polymers with P_m values of 0.66 (Figure 6a) and 0.62, respectively. In contrast, **6**/propan-2-ol and **9**/propan-2-ol, with methyl substituents at the *ortho* and *para* positions of their phenolic groups, furnished atactic materials from *rac*-LA with P_r values of 0.55 and 0.57, respectively. Interestingly, **5**/propan-2-ol afforded heterotactically biased PLAs with a P_r value of 0.64. Heterotactic PLAs cannot be obtained from *rac*-LA through a site control mechanism (SCM) with use of an enantiomeric pure complex, so this reveals the existence of a chain-end control mechanism (CEM) with use of **5**/propan-2-ol in the *rac*-LA polymerization. The heterotacticity of the PLA resulting from *rac*-LA increased to 0.73 when **8**/propan-2-ol was used (Figure 6b), which probably indicates the operation of a propagating chain exchange mechanism as proposed by Coates and co-workers.[9b] In this case, the heteroselectivity of **8**/

Table 2. Polymerization of *rac*- and *meso*-LA in the presence of salan aluminium ethyl compounds **4–9** and propan-2-ol.[a]

LA	Catalyst	t [h]	Conv. [%][b]	$M_{n,\mathrm{calcd}}$[c] $\times 10^3$	$M_{n,\mathrm{GPC}}$[d] $\times 10^3$	$M_{n,\mathrm{NMR}}$[b] $\times 10^3$	PDI	P_m,P_r[e]
rac	**4**	10	70.7	5.09	5.45	5.81	1.09	P_m(0.66)
rac	**5**	57	87.6	6.31	5.59	6.97	1.10	P_r(0.64)
rac	**6**	69	87.0	6.27	6.26	6.03	1.10	P_r(0.55)
meso	**4**	23	97.3	7.01	5.79	6.56	1.12	P_r(0.64)
meso	**5**	27	83.1	5.99	4.38	5.14	1.09	P_r(0.70)
meso	**6**	27	93.5	6.74	5.86	6.91	1.10	P_r(0.69)
rac	**7**	9	89.0	6.41	8.00	8.19	1.12	P_m(0.62)
rac	**8**	34	84.8	6.11	5.59	6.00	1.10	P_r(0.73)
rac	**9**	53	85.5	6.16	5.71	6.05	1.09	P_r(0.57)

[a] All polymerizations were carried out in toluene at 70 °C, $[LA]_0 = 0.534$ M, $[Al]_0 = 10.7$ mM. [b] Determined from ^{1}H NMR. [c] M_n of PLA calculated from $M_n = 144.13 \times 50 \times \mathrm{conv}\,\%$. [d] Determined by GPC (THF), relative to PS standards. The value of M_n was calculated according to $M_n = 0.58\,M_{n,\mathrm{GPC}}$.[33] [e] The parameters P_m and P_r are the probabilities of *meso* and *racemic* enchainments of monomer units, respectively. P_m was calculated from: $[mmm] = P_m^2 + (1-P_m)P_m/2$, $[mmr] = [rmm] = (1-P_m)P_m$, $[rmr] = (1-P_m)^2$, and $[mrm] = [(1-P_m)^2 + P_m(1-P_m)]/2$, and $P_r = 1-P_m$.

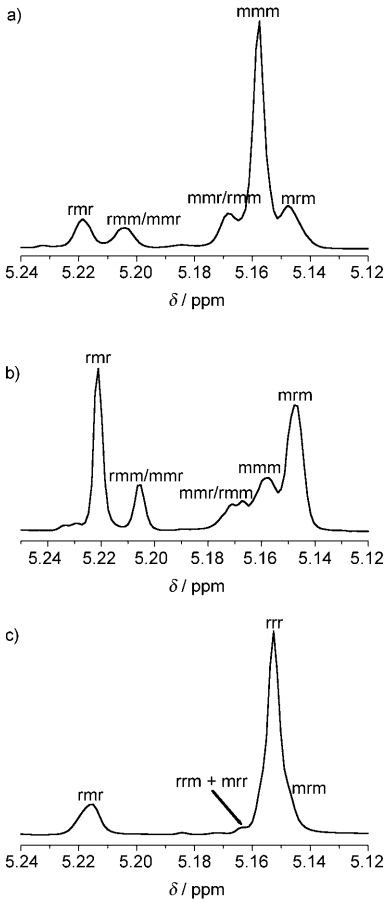

Figure 6. Methine regions of homonuclear decoupled ^{1}H NMR spectra of PLAs produced: from *rac*-LA by use of a) **4**/propan-2-ol, b) **8**/propan-2-ol, and c) from *meso*-LA with **5**/propan-2-ol as catalyst/initiator system.

propan-2-ol should be enhanced relative to that of **5**/propan-2-ol because of a more frequent positive cooperation effect between a CEM and a SCM, resulting from the occurrence of rapid exchange between propagating chains bound to each different enantiomeric ligand before insertion of a subsequent monomer unit (Scheme 3). The **4**/propan-2-ol, **5**/propan-2-ol, and **6**/propan-2-ol systems afforded syndiotactically biased PLAs from *meso*-LA with P_r values of 0.64, 0.70 (Figure 6c), and 0.69, respectively. This clearly confirms the operation of a SCM in *meso*-LA polymerization with use of these chiral complexes.

To gain a better insight into the polymerization mechanism, detailed kinetic studies of *rac*-LA in the presence of **4–6** and **7–9** together with propan-2-ol as initiator were performed. Conversion of *rac*-LA over time at various concentrations of **7**/propan-2-ol in toluene at 70 °C were monitored by ^{1}H NMR spectroscopy ($[LA]_0 = 0.534$ M, $[Al]_0 = 10.7$ to 21.4 mM, and $[LA]_0 = 0.267$ M, $[Al]_0 = 8.9$ mM). In each case, first-order kinetics in monomer were observed and the appropriate semilogarithmic plots are shown in Figure 7a. The polymerization of *rac*-LA in the presence of **7**/propan-2-ol as catalyst/initiator thus proceeds according to:

$$-\mathrm{d}[\mathrm{LA}]/\mathrm{d}t = k_{\mathrm{app}}[\mathrm{LA}] \quad (1)$$

where $k_{\mathrm{app}} = k_{\mathrm{p}}[\mathrm{Al}]^x$, and k_{p} is the propagation rate constant. To determine the order in aluminium (x), k_{app} was plotted against $[Al]_0$ (Figure 7b). In this plot, k_{app} increased linearly with the aluminium concentration, indicating a first order in aluminium (x). Therefore, the polymerization of *rac*-LA in the presence of **7**/propan-2-ol followed the overall kinetic equation:

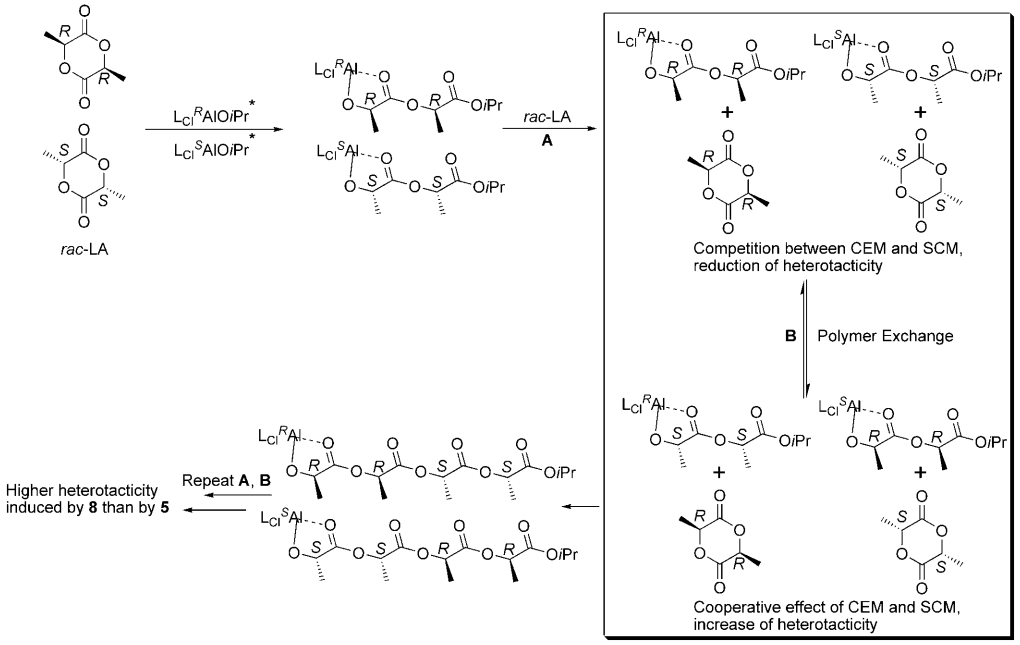

Scheme 3. Proposed polymer exchange mechanism for the explanation of the enhancement of heteroselectivity and activity of **8** compared to **5** (* indicates the aluminium isopropoxides formed by **8** upon addition of propan-2-ol).

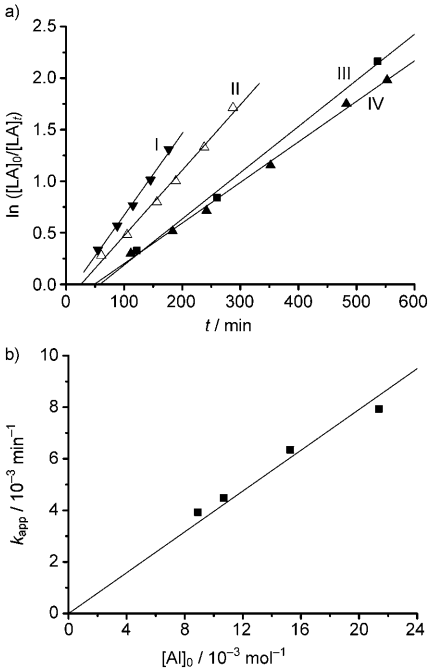

Figure 7. a) First-order kinetic plots for the ROP of *rac*-LA by **7**/propan-2-ol as catalyst/initiator system in toluene at 70 °C with $[LA]_0 = 0.534$ M: I) $[LA]_0/[Al]_0 = 25$; II) $[LA]_0/[Al]_0 = 35$; III) $[LA]_0/[Al]_0 = 50$, $[LA]_0 = 0.267$ M; IV) $[LA]_0/[Al]_0 = 30$. b) Linear plot of k_{app} vs $[Al]_0$ for the polymerization of *rac*-LA with **7**/propan-2-ol as catalyst/initiator system.

$$-\mathrm{d}[LA]/\mathrm{d}t = k_p[Al][LA] \quad (2)$$

A k_p value of $23.8\,M^{-1}h^{-1}$ was calculated (Table 3, entry 3) for *rac*-LA polymerization in the presence of **7**/propan-2-ol in toluene at 70 °C.

Table 3. Kinetic results for *rac*-LA polymerization in the presence of complexes **5**–**9**.[a]

Entry	Complex	k_{app}[b] [$\times 10^{-3}\,h^{-1}$]	k_p[c] [$M^{-1}h^{-1}$]
1	**5**	37.3	3.49
2	**6**	30.8	2.88
3	**7**	269	23.8[d]
4	**8**	56.2	5.26
5	**9**	35.5	3.32

[a] All polymerizations were carried out in toluene at 70 °C, $[LA]_0 = 0.534$ M, $[Al]_0 = 10.7$ mM. [b] Measured by ^{1}H NMR. [c] Calculated from: $k_p = k_{app}/[Al]_0$. [d] Deduced from the linear plot of k_{app} against $[Al]_0$.

Conversion versus time data were also collected for the polymerization of *rac*-LA in the presence of **4**/propan-2-ol (toluene, 70 °C, $[LA]_0 = 0.534$ M, $[Al]_0 = 10.7$ and 17.8 mM, and $[LA]_0 = 0.267$ M, $[Al]_0 = 6.68$ mM). In each case, a significant deviation from a first-order plot for $\ln[LA]_0/[LA]_t$ versus time was observed at high levels of conversion (Figure S5 in the Supporting Information), suggesting a kinetic preference of **4** for a certain lactide enantiomer. The polymerization of (*S*,*S*)- or (*R*,*R*)-LA with application of **4**/propan-2-ol revealed a difference between k_{app} values of one order of magnitude at the same aluminium concentration [(*S*,*S*)-LA: $k_{app} = 517 \times 10^{-3}\,h^{-1}$; (*R*,*R*)-LA: $k_{app} = 51.0 \times 10^{-3}\,h^{-1}$, Figure S6 in the Supporting Information], indicating that **4** has a marked preference for the polymerization of (*S*,*S*)-LA over that of (*R*,*R*)-LA, which is evidence for the operation of a SCM. However, the kinetic resolution ability of **4** for *rac*-LA ($k_{SS}/k_{RR} = 10.1$, Table 4, entry 1) is much lower than that of other reported chiral Schiff base aluminium systems [$k_{RR}/k_{SS} \approx 20$ reported by Spassky for (*R*)-(SalBinap)AlOCH$_3$[9a] and $k_{SS}/k_{RR} \approx 14$ reported by us for (*R*,*R*)-cyclohexylsalen-AlO*i*Pr[9d]). Moreover, the introduction of chlorine atoms or methyl groups both lead to decreased kinetic resolution for **5** and **6** with (*R*,*R*)- and (*S*,*S*)-LA. Unlike **4**, which shows a preference towards (*S*,*S*)-LA, **5** has a preference toward (*R*,*R*)-LA with a k_{SS}/k_{RR} value of 0.62 (Table 4, entry 2, Figure S7), as does **6**, with a k_{SS}/k_{RR} value of 0.82 (Table 4, entry 3, Figure S8).

Table 4. Apparent rate constants for (*S*,*S*)- and (*R*,*R*)-LA polymerizations in the presence of **4**, **5**, and **6** as catalysts and propan-2-ol as an initiator.[a]

Entry	Complex	$k_{app,(S,S)\text{-LA}}$ [$\times 10^{-3}\,h^{-1}$]	$k_{app,(R,R)\text{-LA}}$ [$\times 10^{-3}\,h^{-1}$]	k_{SS}/k_{RR}
1	**4**	517	51.0	10.1
2	**5**	27.5	44.5	0.62
3	**6**	29.0	35.4	0.82

[a] All polymerizations were carried out in toluene at 70 °C, $[LA]_0 = 0.534$ M, $[Al]_0 = 10.7$ mM.

Finally, conversion versus time data were collected for the polymerization of *rac*-LA in the presence of **5**/propan-2-ol or **8**/propan-2-ol and of **6**/propan-2-ol or **9**/propan-2-ol (toluene, 70 °C, $[LA]_0 = 0.534$ M, $[Al]_0 = 10.7$ mM). In each case, first-order kinetics in monomer were observed, and the semilogarithmic plots for these polymerizations are shown in Figure 8a and b, respectively. The k_{app} and k_p values determined are collected in Table 3. The k_{app} and k_p values for **8**/propan-2-ol ($k_p = 5.26\,M^{-1}h^{-1}$) and **9**/propan-2-ol ($k_p = 3.32\,M^{-1}h^{-1}$) are both slightly higher than those for **5** ($k_p = 3.49\,M^{-1}h^{-1}$) and **6** ($k_p = 2.88\,M^{-1}h^{-1}$), respectively, which further confirms a positive cooperation effect between a CEM and a SCM resulting from the occurrence of polymer exchange. The substituents on the salan ligand phenolate rings also affect the polymerization rate significantly. Introducing methyl groups results in a remarkable decrease in k_p from $23.8\,M^{-1}h^{-1}$ for **7** to $3.32\,M^{-1}h^{-1}$ for **9**. The k_p values for **5** and **8** are much lower than the k_p value for **7** ($23.8\,M^{-1}h^{-1}$). This indicates that the introduction of chlorine substituents does not enhance the polymerization rate. Several studies have indicated that electron-withdrawing chlorine substituents on ligands increase Lewis acidities of metal centers, thereby enhancing rates of lactone polymerization.[32] These results indicate that the polymerization rate constant includes several steps, including monomer approach and binding, nucleophilic addition through the metal–alkoxide bond, and rearrangement causing the cleavage of the acyl–oxygen bond. Although the enhancement of the Lewis acidity of the metal center most probably leads to a more facile approach

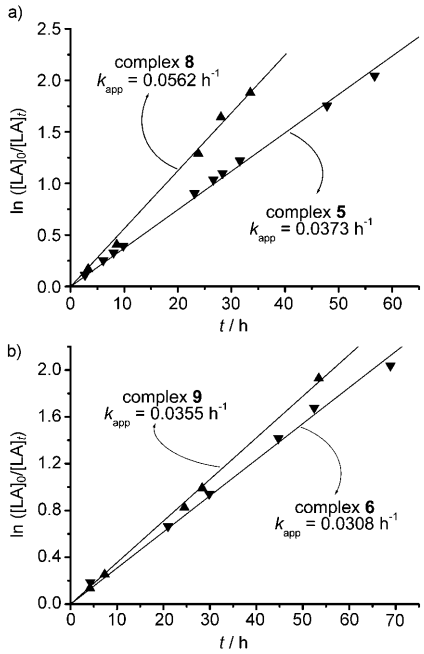

Figure 8. a) First-order kinetic plots for the ROP of *rac*-LA in the presence of **8** or **5** and propan-2-ol in toluene at 70 °C with $[LA]_0 = 0.534$ M, $[Al]_0 = 10.7$ mM. b) First-order kinetic plots for the ROP of *rac*-LA in the presence of **9** or **6** and propan-2-ol in toluene at 70 °C with $[LA]_0 = 0.534$ M, $[Al]_0 = 10.7$ mM.

and binding of the monomer, other changes resulting from the introduction of chlorine atoms may reduce the rates of other steps.

Conclusions

In conclusion, a series of aluminium ethyl complexes ligated by chiral salan ligands has been reported. The structures of two different diastereoisomers—**a** and **b**—of these aluminium ethyl complexes were revealed by ^{1}H NMR and X-ray analysis. Further NMR measurements demonstrated slow exchange between sqp and tbp geometries for diastereoisomers **b** at low temperatures. In the presence of propan-2-ol, the aluminium ethyl complexes acted as efficient initiators for the ROP of *rac*-LA and of *meso*-LA. Microstructural analysis of the resulting polymers and detailed kinetics studies indicate the coexistence of a CEM and a SCM in lactide polymerization. A propagating chain exchange mechanism was proposed in order to explain the enhanced heteroselectivity and activity of **8** towards *rac*-LA polymerization, relative to those of **5**. Furthermore, kinetic analysis revealed first-order kinetics for **7** in both *rac*-LA monomer and catalyst, as well as a kinetic resolution by **4** in favor of (*S*,*S*)-LA. Future work will focus on the separation of diastereoisomers **a** and **b** to explore their different catalytic behavior in lactide polymerization in detail.

Experimental Section

General conditions: All manipulations requiring a dry atmosphere were performed under dry argon by use of standard Schlenk techniques or in a glovebox (M. Braun, Germany). Solvents were dried by heating at reflux over sodium/benzophenone (toluene and hexane) or calcium hydride (propan-2-ol) for at least 24 h. Anhydrous deuterated solvents ([D_8]toluene and [D_6]benzene, Aldrich) were kept under nitrogen over molecular sieves (4 Å). Starting materials for the synthesis of ligand precusors **1–3** were purchased from Aldrich and were used without further purification. The ligands **1–3** were synthesized by literature procedures.[21] Triethylaluminium from Aldrich was used as received. (*S*,*S*)-, *rac*-, and *meso*-LA (Purac Biochem b.v., the Netherlands) were purified by recrystallization three times from anhydrous toluene, followed by drying under vacuum at 30 °C for 24 h before use.

Instruments and measurements: Nuclear magnetic resonance (NMR) spectra were recorded on a Bruker AV 400 MHz instrument at 298 K or a Varian Inova 600 MHz spectrometer at 295 K. [D_1]Chloroform, [D_6]benzene, and [D_8]toluene were used as solvents. Homonuclear decoupled ^{1}H NMR, ^{1}H–^{1}H COSY, ^{1}H–^{1}H NOESY, and diffusion-ordered (DOSY) spectra were recorded on a Bruker Avance II 600 MHz spectrometer operating at 600.13 MHz. The spectrometer was fitted with a Great 3/10 gradient amplifier and a triple-nucleus TXI probe with *z*-gradient. All experiments were performed at 295 K with use of standard pulse sequences from the Bruker library. Pulsed field gradient stimulated echo (PFGSE) diffusion experiments were performed by use of the bipolar stimulated echo sequence with 32 increments in the gradient strength (2–95 %), typically 16 averages per increment step, and 100 ms diffusion time. Levels of monomer conversion were determined from the integrals of signals at 1.65 ppm, representing lactide monomer, and 1.59 ppm, representing PLA. P_m (the probability of *meso* linkages) and P_r values (the probability of *racemic* linkages) were calculated from different tetrad intensities measured by homonuclear decoupled ^{1}H NMR. Gel permeation chromatography (GPC) measurements were conducted with a Waters 410GPC instrument with THF as the eluent (flow rate: 1 mL min^{-1}, 35 °C). The molecular weights were determined relative to polystyrene standards.

Compound (*R*,*R*)-1: ^{1}H NMR (400 MHz, $CDCl_3$, 298 K): $\delta = 10.33$ (br, 2H; ArOH), 7.18 (td, $^4J(H,H) = 1.2$ Hz, $^3J(H,H) = 8.4$ Hz, 2H; ArH), 6.98 (d, $^3J(H,H) = 7.2$ Hz, 2H; ArH), 6.80 (m, 4H; ArH), 3.84 (d, $^2J(H,H) = 13.2$ Hz, 2H; ArCH_2NCH$_3$), 3.64 (d, $^2J(H,H) = 12.9$ Hz, 2H; ArCH_2NCH$_3$), 2.71 (d, $^3J(H,H) = 8.4$ Hz, 2H; CH), 2.23 (s, 6H; NCH$_3$), 2.02 (d, $^2J(H,H) = 10.2$ Hz, 2H; cyclohexane hydrogens), 1.81 (d, $^3J(H,H) = 6.9$ Hz, 2H; cyclohexane hydrogens), 1.15 ppm (m, 4H; cyclohexane hydrogens); ^{13}C NMR (100 MHz, $CDCl_3$, 298 K): $\delta = 157.84$ (ArCOH), 129.03 (ArCH), 128.61 (ArCH), 122.31 (ArCH), 119.03 (Ar*C*CH$_2$), 116.49 (ArCH), 61.91 (cyclohexane carbons), 56.97 (Ar*C*H$_2$NCH$_3$), 35.53 (NCH$_3$), 25.27 (cyclohexane carbons), 22.32 ppm (cyclohexane carbons); elemental analysis calcd (%) for $C_{22}H_{30}N_2O_2$: C 74.54, H 8.53, N 7.90; found: C 74.99, H 8.32, N 7.94.

Compound (*R*,*R*)-2: ^{1}H NMR (400 MHz, [D_6]Me_2SO, 298 K): $\delta = 7.32$ (d, $^4J(H,H) = 2.7$ Hz, 2H; ArH), 7.18 (d, $^4J(H,H) = 2.7$ Hz, 2H; ArH), 3.80 (d, $^2J(H,H) = 13.5$ Hz, 2H; ArCH_2NCH$_3$), 3.56 (d, $^2J(H,H) = 13.2$ Hz, 2H; ArCH_2NCH$_3$), 2.87 (d, $^3J(H,H) = 6.9$ Hz, 2H; CH), 2.14 (s, 6H; NCH$_3$), 1.98 (d, 2H; cyclohexane hydrogens), 1.76 (d, 2H; cyclohexane hydrogens), 1.19 ppm (m, 4H; cyclohexane hydrogens); ^{13}C NMR (100 MHz, [D_6]Me_2SO, 298 K): $\delta = 153.46$ (ArCOH), 128.65 (ArCH), 127.92 (ArCH), 126.97 (ArC), 122.17 (ArC), 120.86 (ArC), 61.96 (cyclohexane carbons), 52.97 (ArCH$_2$NCH$_3$), 35.37 (NCH$_3$), 24.53 (cyclohexane carbons), 22.40 ppm (cyclohexane carbons); elemental analysis calcd (%) for $C_{22}H_{26}Cl_4N_2O_2$: C 53.68, H 5.32, N 5.69; found: C 54.09, H 5.02, N 5.76.

Compound (*R*,*R*)-3: ^{1}H NMR (400 MHz, $CDCl_3$, 298 K): $\delta = 10.00$ (br, 2H; ArOH), 6.78 (s, 2H; ArH), 6.56 (s, 2H; ArH), 3.67 (d, $^2J(H,H) = 13.2$ Hz, 2H; ArCH_2NCH$_3$), 3.50 (d, $^2J(H,H) = 13.2$ Hz, 2H; ArCH_2NCH$_3$), 2.59 (d, $^3J(H,H) = 7.8$ Hz, 2H; CH), 2.14 (s, 6H; NCH$_3$), 2.09 (s, 6H; ArCH$_3$), 2.06 (s, 6H; ArCH$_3$), 1.92 (d, $^3J(H,H) = 8.1$ Hz, 2H; cyclohexane hydrogens), 1.73 (d, 2H; cyclohexane hydrogens), 1.06 ppm

(m, 4H; cyclohexane hydrogens); ^{13}C NMR (100 MHz, $CDCl_3$, 298 K): δ = 153.59 (ArCOH), 130.60 (ArCH), 127.32 ($ArCCH_3$), 127.12 (ArCH), 125.07 ($ArCCH_3$), 121.81 ($ArCCH_2$), 61.46 (cyclohexane carbons), 57.00 ($ArCH_2NCH_3$), 35.31 (NCH_3), 25.32 (cyclohexane carbons), 22.27 (cyclohexane carbons), 20.47 ($ArCH_3$), 15.68 ppm ($ArCH_3$); elemental analysis calcd (%) for $C_{26}H_{38}N_2O_2$: C 76.06, H 9.33, N 6.82; found: C 76.09, H 9.02, N 6.76.

Compound 4: A solution of triethylaluminium in toluene (2.0 M, 2 mL) was added dropwise by syringe at room temperature to a solution of (*R,R*)-**1** (1.42 g, 4 mmol) in toluene (2 mL). Instantaneous evolution of ethane was observed. The colorless reaction mixture was stirred at 70 °C overnight and allowed to cool slowly to room temperature. The solvent was removed under reduced pressure, and the residue was repeatedly washed with anhydrous *n*-hexane to afford the product as colorless crystals (1.09 g, 2.68 mmol, 67 %). The ^{1}H NMR spectra clearly indicated the presence of two complexes. ^{1}H NMR (complex **4a**, 600 MHz, [D_8]toluene, 295 K): δ = 7.17 (dd, ^4J(H,H) = 1.2 Hz, ^3J(H,H) = 7.2 Hz, 2H; ArH), 7.07 (t, ^3J(H,H) = 7.2 Hz, 2H; ArH), 6.84 (t, ^3J(H,H) = 5.4 Hz, 2H; ArH), 6.74 (m, 2H; ArH), 3.70 (d, ^2J(H,H) = 13.0 Hz, 1H; ArCH_2NCH$_3$), 3.60 (d, ^2J(H,H) = 13.0 Hz, 1H; ArCH_2NCH$_3$), 3.19 (d, ^2J(H,H) = 13.0 Hz, 1H; ArCH_2NCH$_3$), 2.71 (d, ^2J(H,H) = 13.0 Hz, 1H; ArCH_2NCH$_3$), 2.29 (td, ^4J(H,H) = 1.2 Hz, ^4J(H,H) = 3.6 Hz, 1H; CH), 2.02 (td, ^4J(H,H) = 1.2 Hz, ^4J(H,H) = 3.6 Hz, 1H; CH), 1.84 (s, 3H; NCH_3), 1.72 (s, 3H; NCH_3), 1.54 (t, 3H; $AlCH_2CH_3$), 1.51 (d, 2H; cyclohexane hydrogens), 1.34 (m, 2H; cyclohexane hydrogens), 0.58 (m, 4H; cyclohexane hydrogens), 0.10 (dq, 1H; $AlCH_2CH_3$), −0.07 ppm (dq, 1H; $AlCH_2CH_3$); ^{1}H NMR (complex **4b**, 600 MHz, [D_8]toluene, 295 K): δ = 7.22 (m, 4H; ArH), 6.90 (dd, ^4J(H,H) = 1.2 Hz, ^3J(H,H) = 7.2 Hz, 2H; ArH), 6.77 (dd, ^4J(H,H) = 1.2 Hz, ^3J(H,H) = 7.2 Hz, 2H; ArH), 3.44 (d, ^2J(H,H) = 13.0 Hz, 2H; ArCH_2NCH$_3$), 3.28 (d, ^2J(H,H) = 13.0 Hz, 2H; ArCH_2NCH$_3$), 2.05 (m, 2H; CH), 1.80 (s, 6H; NCH_3), 1.45 (t, 3H; $AlCH_2CH_3$), 1.41 (d, 2H; cyclohexane hydrogens), 0.78 (m, 2H; cyclohexane hydrogens), 0.67 (m, 4H; cyclohexane hydrogens), 0.23 (dq, 1H; $AlCH_2CH_3$), 0.04 ppm (dq, 1H; $AlCH_2CH_3$); ^{13}C NMR (100 MHz, [D_6]benzene, 298 K): δ = 162.39, 161.75, 131.40, 131.07, 129.56, 129.21, 122.75, 121.06, 120.83, 120.18, 117.32, 116.73, 63.44, 61.55, 60.47, 53.47, 42.74, 36.34, 24.85, 23.48, 22.84, 22.21, 11.99 ppm; elemental analysis calcd (%) for $C_{24}H_{33}AlN_2O_2$: C 70.56, H 8.14, N 6.86; found: C 71.09, H 8.02, N 6.76.

Compound 5: The procedure was similar to that described for **4**, starting with (*R,R*)-**2** (1.97 g, 4 mmol). A white powder was isolated (1.75 g, 3.20 mmol, 80 %). The ^{1}H NMR spectra clearly indicated the presence of two complexes. ^{1}H NMR (complex **5a**, 600 MHz, [D_8]toluene, 295 K): δ = 7.36 (dd, ^4J(H,H) = 2.4 Hz, ^3J(H,H) = 5.4 Hz, 1H; ArH), 7.06 (s, 1H; ArH), 6.66 (dd, ^4J(H,H) = 3.6 Hz, ^3J(H,H) = 5.4 Hz, 2H; ArH), 3.52 (d, ^2J(H,H) = 13.2 Hz, 1H; ArCH_2NCH$_3$), 3.19 (d, ^2J(H,H) = 13.2 Hz, 1H; ArCH_2NCH$_3$), 3.06 (d, ^2J(H,H) = 13.2 Hz, 1H; ArCH_2NCH$_3$), 2.36 (d, ^2J(H,H) = 13.2 Hz, 1H; ArCH_2NCH$_3$), 2.23 (td, 1H; CH), 1.84 (td, 1H; CH), 1.59 (s, 3H; NCH_3), 1.51 (t, 3H; $AlCH_2CH_3$), 1.45 (s, 3H; NCH_3), 1.42 (m, 2H; cyclohexane hydrogens), 1.24 (m, 2H; cyclohexane hydrogens), 0.68–0.48 (m, 4H; cyclohexane hydrogens), −0.10 (dq, 1H; $AlCH_2CH_3$), −0.22 ppm (dq, 1H; $AlCH_2CH_3$); ^{1}H NMR (complex **5b**, 600 MHz, [D_8]toluene, 295 K): δ = 7.38 (d, 2H; ArH), 6.62 (d, 2H; ArH), 2.96 (d, ^2J(H,H) = 13.2 Hz, 2H; ArCH_2NCH$_3$), 2.57 (d, ^2J(H,H) = 13.2 Hz, 2H; ArCH_2NCH$_3$), 2.16 (m, 2H; CH), 1.87 (m, 2H; cyclohexane hydrogens), 1.62 (s, 6H; NCH_3), 1.32 (t, 3H; $AlCH_2CH_3$), 1.17 (m, 2H; cyclohexane hydrogens), 0.76 (m, 4H; cyclohexane hydrogens), 0.05 (dq, 1H; $AlCH_2CH_3$), −0.16 ppm (dq, 1H; $AlCH_2CH_3$); ^{13}C NMR (100 MHz, [D_6]benzene, 298 K): δ = 156.02, 155.55, 130.64, 130.52, 127.84, 127.56, 126.26, 126.13, 124.43, 123.30, 121.53, 120.08, 63.74, 62.06, 59.51, 58.63, 42.96, 35.83, 24.53, 23.40, 22.81, 22.57, 11.43, 0.86 ppm; elemental analysis calcd (%) for $C_{24}H_{29}AlCl_4N_2O_2$: C 52.77, H 5.35, N 5.13; found: C 52.56, H 5.58, N 5.76.

Compound 6: The procedure was similar to that described for **4**, starting from (*R,R*)-**3** (4.10 g, 10 mmol). A white powder was isolated (3.35 g, 7.20 mmol, 72 %). The ^{1}H NMR spectra clearly indicated the presence of two complexes. ^{1}H NMR (complex **6a**, 600 MHz, [D_8]toluene, 295 K): δ = 7.02 (d, ^2J(H,H) = 12.0 Hz, 2H; ArH), 6.56 (d, ^3J(H,H) = 6.0 Hz, 2H; ArH), 3.71 (d, ^2J(H,H) = 12.0 Hz, 1H; ArCH_2NCH$_3$), 3.66 (d, ^2J(H,H) = 12.0 Hz, 1H; ArCH_2NCH$_3$), 3.27 (d, ^2J(H,H) = 12.0 Hz, 1H; ArCH_2NCH$_3$), 2.70 (d, ^2J(H,H) = 12.0 Hz, 1H; ArCH_2NCH$_3$), 2.60 (s, 3H; $ArCH_3$), 2.46 (s, 3H; $ArCH_3$), 2.36 (s, 6H; $ArCH_3$), 2.01 (td, 1H; cyclohexane hydrogens), 1.89 (s, 3H; NCH_3), 1.73 (s, 3H; NCH_3), 1.57 (t, 3H; $AlCH_2CH_3$), 1.39 (m, 4H; cyclohexane hydrogens), 0.62 (m, 4H; cyclohexane hydrogens), 0.06 (dq, 1H; $AlCH_2CH_3$), −0.05 ppm (dq, 1H; $AlCH_2CH_3$); ^{1}H NMR (complex **6b**, 600 MHz, [D_8]toluene, 295 K): δ = 7.03 (s, 2H; ArH), 6.64 (s, 2H; ArH), 3.46 (br, 2H; ArCH_2NCH$_3$), 3.32 (d, ^2J(H,H) = 12.0 Hz, 2H; ArCH_2NCH$_3$), 2.59 (s, 6H; $ArCH_3$), 2.34 (s, 6H; $ArCH_3$), 2.09 (m, 2H; CH), 1.79 (s, 6H; NCH_3), 1.44 (t, 3H; $AlCH_2CH_3$), 1.37 (m, 4H; cyclohexane hydrogens), 0.65 (m, 4H; cyclohexane hydrogens), 0.21 (dq, 1H; $AlCH_2CH_3$), 0.20 ppm (dq, 1H; $AlCH_2CH_3$); ^{13}C NMR (100 MHz, [D_6]benzene, 298 K): δ = 157.08, 156.45, 131.79, 131.59, 131.41, 126.85, 126.48, 124.25, 122.84, 62.84, 61.17, 59.42, 53.16, 42.09, 35.19, 24.30, 22.69, 22.20, 21.76, 16.29, 11.50, 11.12 ppm; elemental analysis calcd (%) for $C_{28}H_{41}AlN_2O_2$: C 72.38, H 8.89, N 6.03; found: C 72.09, H 9.02, N 6.26.

General procedure for lactide polymerization: In a typical polymerization experiment, *rac*-LA (1.00 g, 6.94 mmol), **4** (0.057 g, 0.14 mmol), propan-2-ol (8.41 mg, 0.14 mmol in toluene, 4 mL), and additional toluene (9 mL) were introduced successively into a flame-dried vessel containing a magnetic bar. The vessel was placed in an oil bath thermostated at 70 °C. After certain time intervals, aliquots were taken out for determination of the level of monomer conversion by ^{1}H NMR. The polymer was isolated by precipitation into cold methanol. The precipitate was collected and dried under vacuum at 40 °C for 24 h.

X-ray crystallographic studies: Suitable single crystals of **4a** and **9a** were grown from saturated toluene solutions at room temperature. The intensity data were collected from the ω scan mode (187 K) on a Bruker Smart APEX diffractometer with a CCD detector with use of $Mo_{K\alpha}$ radiation (λ = 0.71073 Å). The crystal structures were solved by use of the SHELXTL program by means of direct methods; the remaining atoms were located from the difference Fourier synthesis, followed by full-matrix, least-squares refinements. The positions of the hydrogen atoms were calculated theoretically and included in the final cycles of refinements in a riding model along with attached carbons. The molecular structures of **4a** and **9a** are shown in Figures 2 and 5, respectively, and their main crystallographic data are summarized in Table 1.

CCDC 632143 and 628811 contain the supplementary crystallographic data for this paper. These data can be obtained free of charge from The Cambridge Crystallographic Data Centre via www.ccdc.cam.ac.uk/data_request/cif

Acknowledgements

The authors thank the Chinese Academy of Sciences and the Royal Netherlands Academy of Arts and Sciences for funding of the CAS-KNAW joint training PhD program (06PhD09). A.H.V acknowledges the Dutch nanotechnology program NanoNed and J. Sun acknowledges the National Natural Science Foundation of China (NSFC) project (20604030) for financial support.

[1] a) B. Jeong, Y. H. Bae, D. S. Lee, S. W. Kim, *Nature* **1997**, *388*, 860; b) K. E. Uhrich, S. M. Cannizzaro, R. S. Langer, K. M. Shakesheff, *Chem. Rev.* **1999**, *99*, 3181; c) Y. Kikkawa, H. Abe, T. Iwata, Y. Inoue, Y. Doi, *Biomacromolecules* **2002**, *3*, 350; d) A. Finne, A.-C. Albertsson, *Biomacromolecules* **2003**, *4*, 684.

[2] a) B. J. O'Keefe, M. A. Hillmyer, W. B. Tolman, *J. Chem. Soc. Dalton Trans.* **2001**, 2215; b) O. Dechy-Cabaret, B. Martin-Vaca, D. Bourissou, *Chem. Rev.* **2004**, *104*, 6147; c) M. H. Chisholm, Z. P. Zhou, *J. Mater. Chem.* **2004**, *14*, 3081; d) Z. Zhong, P. J. Dijkstra, J. Feijen, *J. Biomater. Sci. Polym. Ed.* **2004**, *15*, 929; e) J. Wu, T.-L. Yu, C.-T. Chen, C.-C. Lin, *Coord. Chem. Rev.* **2006**, *250*, 602.

[3] a) M. H. Chisholm, J. C. Gallucci, K. Phomphrai, *Inorg. Chem.* **2004**, *43*, 6717; b) Z. Zhong, S. Schneiderbauer, P. J. Dijkstra, M. Westerhausen, J. Feijen, *Polym. Bull.* **2003**, *51*, 175; c) M. H. Chisholm, J.

Gallucci, K. Phomphrai, *Chem. Commun.* **2003**, 48; d) H.-Y. Chen, H.-Y. Tang, C.-C. Lin, *Polymer* **2007**, *48*, 2257.

[4] a) H. Li, C. Wang, F. Bai, J. Yue, H.-G. Woo, *Organometallics* **2004**, *23*, 1411; b) S. Doherty, R. J. Errington, N. Housley, W. Clegg, *Organometallics* **2004**, *23*, 2382; c) H. Ma, G. Melillo, L. Oliva, T. P. Spaniol, U. Englert, J. Okuda, *J. Chem. Soc. Dalton Trans.* **2005**, 721; d) B. Lian, C. M. Thomas, O. L. Casagrande, C. W. Lehmann, T. Roisnel, J.-F. Carpentier, *Inorg. Chem.* **2007**, *46*, 328.

[5] a) M. H. Chisholm, N. W. Eilerts, J. C. Huffman, S. S. Iyer, M. Pacold, K. Phomphrai, *J. Am. Chem. Soc.* **2000**, *122*, 11845; b) M. S. Hill, P. B. Hitchcock, *J. Chem. Soc. Dalton Trans.* **2002**, 4694; c) D. Chakraborty, E. Y.-X. Chen, *Organometallics* **2003**, *22*, 769; d) C. K. Williams, L. E. Breyfogle, S. K. Choi, W. Nam, V. G. Young, M. A. Hillmyer, W. B. Tolman, *J. Am. Chem. Soc.* **2003**, *125*, 11350; e) A. P. Dove, V. C. Gibson, E. L. Marshall, A. J. P. White, D. J. Williams, *J. Chem. Soc. Dalton Trans.* **2004**, 570; f) T. Chivers, C. Fedorchuk, M. Parvez, *Organometallics* **2005**, *24*, 580; g) J. Ejfler, M. Kobylka, L. B. Jerzykiewicz, P. Sobota, *J. Chem. Soc. Dalton Trans.* **2005**, 2047; h) B.-H. Huang, C.-N. Lin, M.-L. Hsueh, T. Athar, C.-C. Lin, *Polymer* **2006**, *47*, 6622.

[6] a) Y. Kim, J. G. Verkade, *Organometallics* **2002**, *21*, 2395; b) Y. Takashima, Y. Nakayama, K. Watanabe, T. Itono, N. Ueyama, A. Nakamura, H. Yasuda, A. Harada, *Macromolecules* **2002**, *35*, 7538; c) C. K. A. Gregson, I. J. Blackmore, V. C. Gibson, N. J. Long, E. L. Marshall, A. J. P. White, *J. Chem. Soc. Dalton Trans.* **2006**, 3134; d) J. Ejfler, M. Kobylka, L. B. Jerzykiewicz, P. Sobota, *J. Mol. Catal. A* **2006**, *257*, 105.

[7] a) V. C. Gibson, E. L. Marshall, D. Navarro-Llobet, A. J. P. White, D. J. Williams, *J. Chem. Soc. Dalton Trans.* **2002**, 4321; b) B. J. O'Keefe, L. E. Breyfogle, M. A. Hillmyer, W. B. Tolman, *J. Am. Chem. Soc.* **2002**, *124*, 4384.

[8] a) H. Ma, T. P. Spaniol, J. Okuda, *J. Chem. Soc. Dalton Trans.* **2003**, 4770; b) H. Ma, J. Okuda, *Macromolecules* **2005**, *38*, 2665; c) I. Westmoreland, J. Arnold, *J. Chem. Soc. Dalton Trans.* **2006**, 4155; d) Y. Yang, S. Li, D. Cui, X. Chen, X. Jing, *Organometallics* **2007**, *26*, 671.

[9] For the formation of isotactic or stereoblock PLAs, see: a) N. Spassky, M. Wisniewski, C. Pluta, A. Le Borgne, *Macromol. Chem. Phys.* **1996**, *197*, 2627; b) T. M. Ovitt, G. W. Coates, *J. Am. Chem. Soc.* **2002**, *124*, 1316; c) Z. Zhong, P. J. Dijkstra, J. Feijen, *Angew. Chem.* **2002**, *114*, 4692; *Angew. Chem. Int. Ed.* **2002**, *41*, 4510; d) Z. Zhong, P. J. Dijkstra, J. Feijen, *J. Am. Chem. Soc.* **2003**, *125*, 11291; e) N. Nomura, R. Ishii, M. Akakura, K. Aoi, *J. Am. Chem. Soc.* **2002**, *124*, 5938; f) Z. Tang, X. Chen, X. Pang, Y. Yang, X. Zhang, X. Jing, *Biomacromolecules* **2004**, *5*, 965; g) Z. Tang, X. Chen, Y. Yang, X. Pang, J. Sun, X. Zhang, X. Jing, *J. Polym. Sci., Part A: Polym. Chem.* **2004**, *42*, 5974; h) R. Ishii, N. Nomura, T. Kondo, *Polym. J.* **2004**, *36*, 261; i) P. Hormnirum, E. L. Marshall, V. C. Gibson, R. I. Pugh, A. J. P. White, *Proc. Natl. Acad. Sci. USA* **2006**, *103*, 15343; j) A. P. Dove, H. Li, R. C. Pratt, B. G. G. Lohmeijer, D. A. Culkin, R. M. Waymouth, J. L. Hedrick, *Chem. Commun.* **2006**, 2881; k) L. Zhang, F. Nederberg, J. M. Messman, R. C. Pratt, J. L. Hedrick, C. G. Wade, *J. Am. Chem. Soc.* **2007**, *129*, 12610; l) N. Nomura, R. Ishii, Y. Yamamoto, T. Konda, *Chem. Eur. J.* **2007**, *13*, 4433; m) M. Bouyahyi, E. Grunova, N. Marquet, E. Kirillov, C. M. Thomas, T. Roisnel, J.-F. Carpentier, *Chem. Eur. J.* **2008**, *14*, 5815.

[10] For the formation of heterotactic PLAs, see: a) B. M. Chamberlain, M. Cheng, D. R. Moore, T. M. Ovitt, E. B. Lobkovsky, G. W. Coates, *J. Am. Chem. Soc.* **2001**, *123*, 3229; b) M. H. Chisholm, J. C. Huffman, K. Phomphrai, *J. Chem. Soc. Dalton Trans.* **2001**, 222; c) M. H. Chisholm, J. Gallucci, K. Phomphrai, *Inorg. Chem.* **2002**, *41*, 2785; d) M. H. Chisholm, J. C. Gallucci, K. Phomphrai, *Inorg. Chem.* **2004**, *43*, 6717; e) T. R. Jensen, L. E. Breyfogle, M. A. Hillmyer, W. B. Tolman, *Chem. Commun.* **2004**, 2504; f) H.-Y. Chen, H.-Y. Tang, C.-C. Lin, *Macromolecules* **2006**, *39*, 3745; g) H. Ma, T. P. Spaniol, J. Okuda, *Angew. Chem.* **2006**, *118*, 7982; *Angew. Chem. Int. Ed.* **2006**, *45*, 7818; h) A. J. Chmura, C. J. Chuck, M. G. Davidson, M. D. Jones, M. D. Lunn, S. D. Bull, *Angew. Chem.* **2007**, *119*, 2330; *Angew. Chem. Int. Ed.* **2007**, *46*, 2280; and references [9b,j,12,13].

[11] For the formation of syndiotactic PLAs, see references [9b,10a,12b].

[12] a) C.-X. Cai, A. Amgoune, G. W. Lehmann, J.-F. Carpentier, *Chem. Commun.* **2004**, 330; b) A. Amgoune, C. M. Thomas, T. Roisnel, J.-F. Carpentier, *Chem. Eur. J.* **2006**, *12*, 169; c) A. Amgoune, C. M. Thomas, J.-F. Carpentier, *Macromol. Rapid Commun.* **2007**, *28*, 693.

[13] X. Liu, X. Shang, T. Tang, N. Hu, F. Pei, D. Cui, X. Chen, X. Jing, *Organometallics* **2007**, *26*, 2747.

[14] D. A. Atwood, J. Benson, J. A. Jegier, N. F. Lindholm, K. J. Martin, R. A. Pitura, D. Rutherford, *Main Group Chem.* **1995**, *1*, 99.

[15] H. Egami, T. Katsuki, *J. Am. Chem. Soc.* **2007**, *129*, 8940.

[16] H. Egami, T. Katsuki, *Synlett* **2008**, 1543.

[17] K. P. Bryliakov, E. P. Talsi, *Eur. J. Org. Chem.* **2008**, 3369.

[18] J. Sun, C. Zhu, Z. Dai, M. Yang, Y. Pan, H. Hu, *J. Org. Chem.* **2004**, *69*, 8500.

[19] Z. Dai, C. Zhu, M. Yang, Y. Zheng, Y. Pan, *Tetrahedron: Asymmetry* **2005**, *16*, 605.

[20] Z. Dai, M. Shao, X. Hou, C. Zhu, Y. Zhu, Y. Pan, *Appl. Catal. A* **2005**, *19*, 898.

[21] A. Yeori, S. Groysman, I. Goldberg, M. Kol, *Inorg. Chem.* **2005**, *44*, 4466.

[22] H. Yang, H. Wang, C. Zhu, *J. Org. Chem.* **2007**, *72*, 10029.

[23] A. Yeori, I. Goldberg, M. Shuster, M. Kol, *J. Am. Chem. Soc.* **2006**, *128*, 13062.

[24] S. Segal, A. Yeori, M. Shuster, Y. Rosenberg, M. Kol, *Macromolecules* **2008**, *41*, 1612.

[25] Achiral salan aluminium methyl complexes and their application in *rac*-LA polymerization has been reported: P. Hormnirum, E. L. Marshall, V. C. Gibson, A. J. P. White, D. J. Williams, *J. Am. Chem. Soc.* **2004**, *126*, 2688.

[26] J. F. Larrow, E. N. Jacobsen, Y. Gao, Y. Hong, X. Nie, C. M. Zepp, *J. Org. Chem.* **1994**, *59*, 1939.

[27] a) A. W. Addison, T. N. Rao, J. Reedijk, J. Van Rijn, G. C. Verschoor, *J. Chem. Soc. Dalton Trans.* **1984**, 1349; b) D. A. Atwood, M. S. Hill, J. A. Jegier, D. Rutherford, *Organometallics* **1997**, *16*, 2659.

[28] J. P. Duxbury, J. N. D. Warne, R. Mushtaq, C. Ward, M. Thornton-Pett, M. Jiang, R. Greatrex, T. P. Kee, *Organometallics* **2000**, *19*, 4445.

[29] D. A. Atwood, *Coord. Chem. Rev.* **1997**, *165*, 267.

[30] a) J. W. Akitt, R. H. Duncan, *J. Magn. Reson.* **1974**, *15*, 162; b) O. Kriz, B. Casensky, A. Lycka, J. Fusek, S. Hermanek, *J. Magn. Reson.* **1984**, *60*, 375.

[31] N. Nomura, T. Aoyama, R. Ishii, T. Kondo, *Macromolecules* **2005**, *38*, 5363.

[32] a) P. A. Cameron, D. Jhurry, V. C. Gibson, A. J. P. White, D. J. Williams, S. Williams, *Macromol. Rapid Commun.* **1999**, *20*, 616; b) D. Jhurry, A. Bhaw-Luximon, N. Spassky, *Macromol. Symp.* **2001**, *175*, 67; c) H. Du, X. Pang, H. Yu, X. Zhuang, X. Chen, D. Cui, X. Wang, X. Jing, *Macromolecules* **2007**, *40*, 1904.

[33] J. Baran, A. Duda, A. Kowalski, R. Szymanski, S. Penczek, *Macromol. Rapid Commun.* **1997**, *18*, 325.

Received: March 27, 2009
Published online: August 18, 2009

